NONLINEAR DYNAMICS ON PARAMETRIC ROLL RESONANCE WITH REALISTIC NUMERICAL MODELLING

Naoya Umeda*, Hirotada Hashimoto*, Dracos Vassalos**, Shinichi Urano* and Kenji Okou*
* Department of Naval Architecture and Ocean Engineering, Osaka University, (Japan)
**Department of Naval Architecture and Marine Engineering, Universities of Glasgow and Strathclyde,(the United Kingdom)

Abstract

This paper describes latest collaborative researches between Japan and the UK on parametric roll resonance of a container ship in following and head seas with realistic modelling of restoring moment as a nonlinear function of wave steepness in experimental, geometrical and analytical approaches. Firstly, captive model experiments were conducted, and demonstrated that the Froude-Krylov prediction could overestimate the amplitude of its variation. Secondly, Poincare mapping technique applied to the numerical model with measured time-varying restoring moment was used for tracing stable steady states, and revealed symmetry-breaking, period-doubling, chaos and capsizing associated with parametric roll resonance. Thirdly, an averaging method was applied to the same numerical model, and confirmed good agreement with the Poincare mapping as well as subcritical bifurcation. Finally, by utilising the present numerical model and methodology, it is shown that a requirement of higher metacentric height does not always improve safety for capsizing associated with parametric roll resonance.

1. INTRODUCTION

Parametric roll resonance is a ship roll motion induced by a time-varying restoring arm as a parameter in equations of motions. Here the roll frequency is multiple of half of the encounter frequency and is nearly equal to the natural roll frequency. In case the roll frequency is half of the encounter frequency, this roll motion could be so significant that a ship could even capsize, and is called as low cycle resonance or principal resonance. The reason why the restoring arm changes with time is that the water plane area changes with relative wave elevation. Because of flare at the bow and transom stern, this change can be significant in longitudinal waves.

Although this phenomenon is well known among theoretical researchers, it has been regarded as rather an exceptional event in actual ocean waves, e.g. short-crested irregular waves. However, a recent model experiment showed that a container ship complying with the Intact Stability Code (IS Code) of the International Maritime Organization (IMO) could suffer severe parametric rolling even in short-crested irregular following waves and could capsize in long-crested irregular following waves. [1] Moreover, severe parametric rolling in head seas at the Pacific Oceans was reported for a post-Panamax C11

class container ship. [2] The former forced to describe parametric rolling in the IMO operational guidance, MSC Circ. 707, and the latter resulted in the review of the IMO IS Code to open a door to a performance-based criteria instead of existing prescriptive criteria. [3] For this purpose, prediction of parametric rolling is required to have quantitative accuracy and identify all potential danger.

Theoretical works on parametric roll resonance can be found in the thirties with linear restoring. [4] Later, in the fifties, linear and nonlinear damping was taken into account. [5] These studies enable us to discuss parametric roll resonance with the Mathieu equation. Then, to investigate capsizing, nonlinearity of restoring moment in still water was taken into account. At this stage, nonlinear dynamical system approach including geometrical and analytical studies is required to identify all potential danger among co-existing states. Such examples can be found in Sanchez and Nayfeh [6], Kan and Taguchi [7], Soliman and Thompson [8] for uncoupled roll models and Oh et al. [9] for coupled pitch-roll model. These theoretical studies focused on understanding fundamental mechanism of the phenomena with rather simplified mathematical modelling. For example, the amplitude of restoring arm is often provided a priori without any relationship with wave steepness or exciting moment.

On the other hand, several six degrees-of-freedom model such as Munif et al. [10] have been developed for quantitative numerical prediction in time domain. Here the relationship between wave steepness and restoring moment is fully taken into account. However, the works using these detailed models only show simulated results with limited number of initial condition sets. Because of nonlinearity of the system, there is a possibility to overlook some potential danger.

Considering the above, we can conclude that a certain gap between the nonlinear dynamic approach based on simplified models and numerical studies without any care of initial condition assemblies. Obviously both of them are insufficient for the purpose of performance-based criteria.

Therefore, the authors intend to bridge this gap by applying nonlinear dynamics into realistic mathematical modelling. This paper overviews a first step in this direction. Here the system is limited to an uncoupled roll motion but the restoring moment modelled as the function of wave steepness with either captive model experiment or conventional theoretical prediction. The nature of parametric roll resonance is discussed with both geometrical and analytical approaches. Furthermore, head sea parametric rolling is also mentioned together with the applicability of the container ship criteria of the IMO IS Code.

2. CAPTIVE MODEL EXPERIMENT ON ROLL RESTORING MOMENT

It is well accepted that wave effect on roll restoring moment can be qualitatively estimated with the Froude-Krylov assumption. [11-13] However, some of the authors [14] reported that the Froude-Krylov prediction could overestimate for a fishing vessel known as the ITTC Ship A-2 [15] as a result of captive model experiments. Thus we conducted captive model experiments for a container ship known as the ITTC Ship A-1 [15], which is more relevant to parametric roll resonance. Its principal particulars and body plan are shown in Table 1 and Fig. 1, respectively. This ship has larger beam-to-length ratio than the post-Panamax C11 class container ship but its bow flare and transom stern are not so exaggerated.

The experiment was carried out with its 1/60 scaled model in the Towing Tank of Osaka University, which is 100 metres in long, 7.8 metres in wide and 4.35 metres in deep. The model was attached to a towing carriage with the heel angles of both 0 and 10 degrees, and free in heave and pitch. The surge force, sway force, yaw moment and roll moment were measured by a dynamometer. The metacentric height (GM) were obtained as the difference of the measured roll moment between 0 degrees and 10 degrees, and then its amplitude, phase-lag and average were identified by the Fourier expansion of measured time series. Regular wave trains were generated by a plunger-type wave maker and their wave length used in these experiments were equal to the ship length.

Table 1 Principal particulars of the subject ship

Items	*Tested ship*
length : L_{pp}	150.0 m
breadth : B	27.2 m
depth : D	13.5 m
draught at FP : T_f	8.5 m
Mean draught : T	8.5 m
draught at AP : T_a	8.5 m
Block coefficient : C_b	0.667
Pitch radius of gyration : κ_{yy}/L_{pp}	0.244
longitudinal position of centre of gravity from the midship : x_{CG}	1.01 m aft
metacentric height : GM	0.15 m
natural roll period : T_ϕ	43.3 s

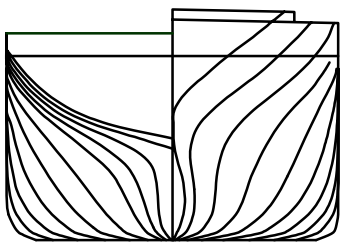

Fig. 1 Body plan of the subject ship

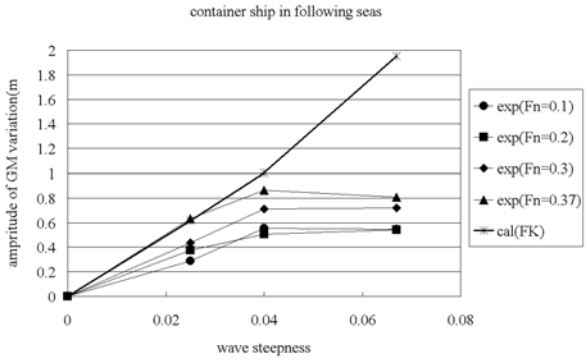

Fig. 2 Amplitude of the metacentric height variation in following seas.

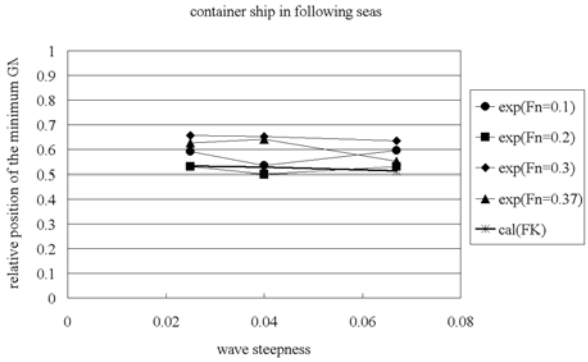

Fig. 3 Relative position of the minimum metacentric height in following seas.

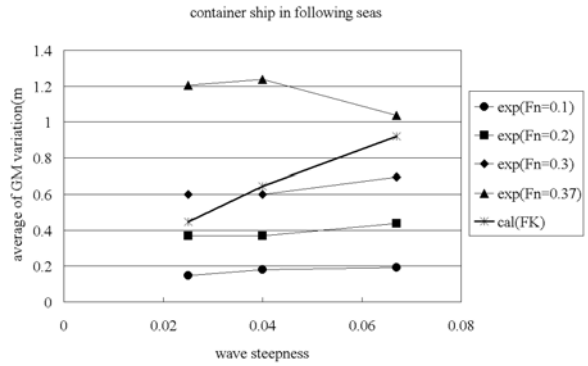

Fig. 4 Average of the metacentric height variation in following seas.

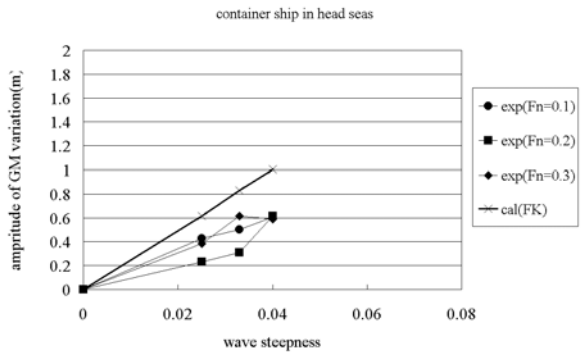

Fig. 5 Amplititude of the metacentric height variation in head seas.

The obtained results from the experiments in following seas are compared with the calculation based on the Froude-Krylov assumption as shown in Figs. 2-4. Here the calculation was obtained by integrating undisturbed wave pressure up to the wave surface with the Smith effect for a ship free in heave and pitch. [12] Thus the calculated results do not depend on the Froude number. In case of following seas, while the relationship between the calculated results and the wave steepness is almost linear, the measured results show some nonlinearity beyond the wave steepness of 0.04. This is probably because hydrodynamic pressure due to shipping water observed at such Froude number induced additional heel moment. When the Froude number of 0.37, at which the encounter frequency is close to zero, the measured values agree well with the calculated ones. However, when the Froude number decreases, the measured values decrease. Thus, we can conclude that the Froude-Krylov calculation overestimates the measured values at low speed cases, where parametric rolling occurs. As the relative position of the minimum GM, which is defined as the horizontal distance of the ship centre from a wave trough divided by the wave length, both the experiment and the calculation indicate wave crests. For the average of GM variation due to waves, measured values clearly depend on the Froude number while the calculated ones do not. Similar outcomes were found in head sea cases as shown in Fig. 5. Thus, it is necessary to model the amplitude and the average of GM variation due to waves as functions of wave steepness, preferably from the captive model experiments. More details of this comparison study will be published in a separate paper.

3. GEOMETRICAL APPROACH

Based on the conclusion from the captive experiments, an equation of the uncoupled roll motion, ϕ, is provided as follows:

$$\begin{aligned}\ddot{\phi} + 2\alpha\dot{\phi} + \gamma\dot{\phi}^3 + \omega_\phi^2\phi + \omega_\phi^2\{(\zeta_{ae}q_1 + \zeta_{ae}^2 q_2 + \zeta_{ae}^3 q_3) \\ + (\zeta_{ae}p_1 + \zeta_{ae}^2 p_2)\cos\omega_e t\}\{\phi - (1/\pi^2)\phi^3\} \\ + \omega_\phi^2 l_3\phi^3 + \omega_\phi^2 l_5\phi^5 = \zeta_a rk\omega_\phi^2 \sin\chi \sin\omega_e t\end{aligned} \quad (1)$$

where α and γ are linear and cubic roll damping coefficients; ω_ϕ and ω_e are the natural and encounter frequencies, respectively; ζ_a is wave amplitude; k is wave number; r is effective wave slope coefficient; χ is heading angle from the wave direction; l_3 and l_5 are the constant coefficients of restoring moment in calm water; q_1, q_2, q_3, p_1 and p_2 are the constant coefficients of the wave effect on restoring moment. And ζ_{ae} is Grim's effective wave defined as follows:

$$\zeta_{ae} = \zeta_a \sqrt{\frac{2\pi\frac{L}{\lambda}\cos(\chi)\sin\left(\pi\frac{L}{\lambda}\cos(\chi)\right)}{\pi^2 - \left(\pi\frac{L}{\lambda}\cos(\chi)\right)^2}} \quad (2)$$

where λ is the wave length; L is the ship length. [16]

This equation is simplified from the coupled surge-sway-yaw-roll model developed by the authors [14]. The degrees of freedom are planed to increase as the next step in future.

Numerical simulation was carried out to trace

steady states. Once a steady state for a certain wave steepness is found, the numerical integration of the equation (1) starts from the steady state but with slightly different wave steepness, say 0.001. Ignoring the first 100 cycles as a transient state, the roll angle as the Poincare map [17] for the next 50 cycles are plotted. Here the Poincare section is set to the wave crests at the centre of ship mass. Both the cases of increasing and decreasing wave steepness were explored. The wave length-to-ship length ratio is 1.5. Here the restoring arm curves in still water and extinction curves are modelled as shown in Figs.6-7, respectively. Under this condition, the parametric roll resonance is expected at the Froude number of about 0.2 in following seas.

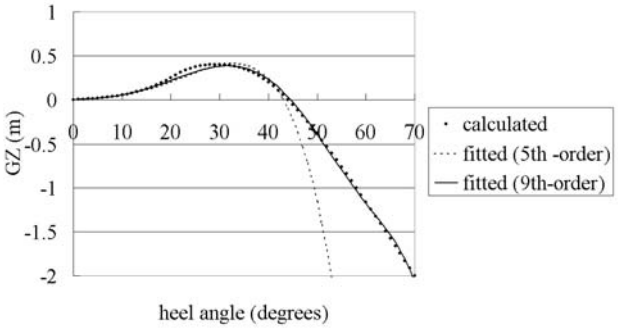

Fig. 6 Restoring arm curves in calm water

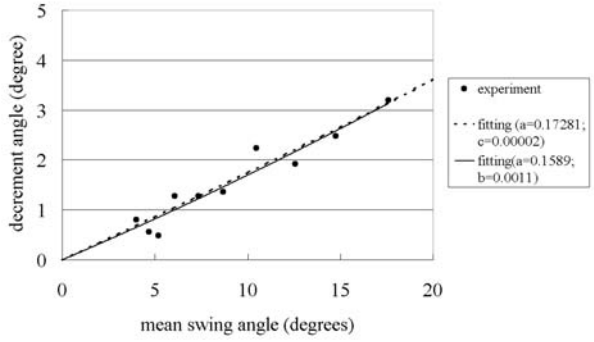

Fig. 7 Extinction curves. Here *a, b, c* are linear, quadratic and cubic extinction coefficients, respectively.

Numerical results for the case of the Froude number of 0.2 are shown in Fig. 8. When the wave steepness is low enough, no roll motion occurs. When the wave steepness exceeds 0.014, the large roll motion suddenly appears with period twice that of sampling, e.g. a period-2 orbit. In addition, as shown in Fig.9, its period is nearly equal to the natural roll period. Thus, this is parametric rolling. If the wave steepness further increases, the amplitude of the parametric rolling decreases and disappears at the wave steepness of 0.044. And then parametric rolling restarts at the wave steepness of 0.056. When the wave steepness increases further, symmetry breaking of parametric rolling occurs. Here, as shown in Fig. 10, a period-1 orbit is superimposed on a period-2 orbit. If a period-1 orbit exists in Eq. (1), some bias can theoretically appear as a product of the period-1 roll motion and the period-1 restoring arm. If the wave steepness further increases from this situation, chaos attractor is observed. Here the Poincare point is not discrete and the phase trajectory shown in Fig.11 becomes complicated. When the wave steepness slightly increases from this wave steepness, capsizing occurs. Here, as shown in Fig. 12, period-1 and period-2 cycles almost alternatively appear and finally capsizing occurs as a part of period-2. If we decrease the wave steepness from chaotic attractor, similar result can be obtained but the wave steepness that parametric rolling suddenly disappears is lower than the wave steepness that parametric rolling suddenly emerges in the case of forward sweeping. This means that parametric rolling could include hysteresis and different steady states could be realised with different initial conditions.

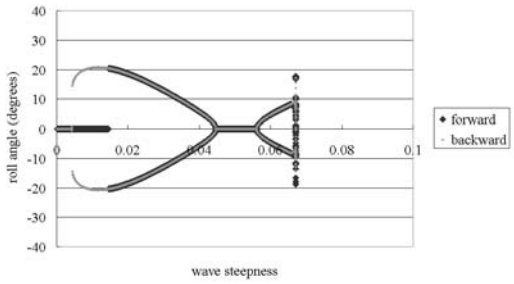

Fig. 8 Roll angles obtained by Poincare mapping with the time-varying restoring moment calculated with the Froude-Krylov assumption.

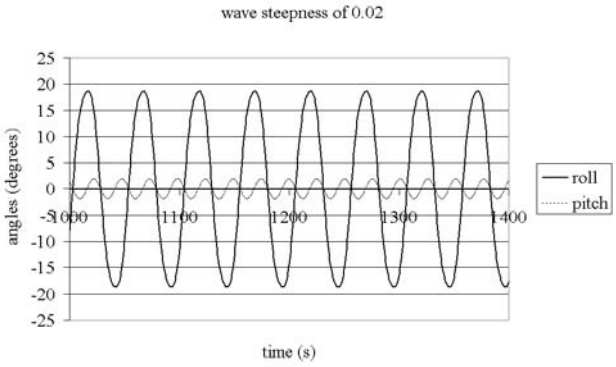

Fig. 9 Time series for the wave steepness of 0.02

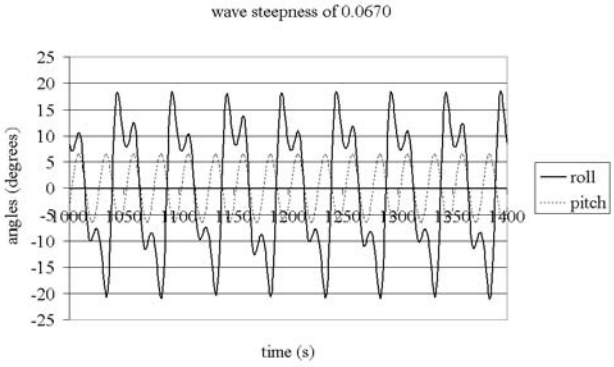

Fig. 10 Time series for the wave steepness of 0.0670

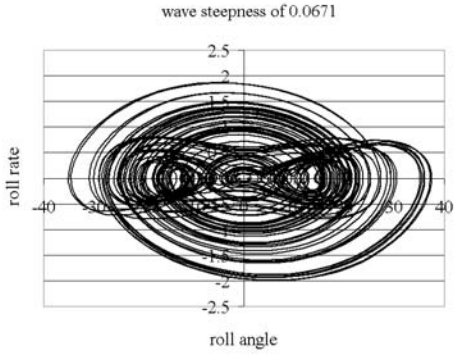

Fig. 11 Phase trajectory for the wave steepness of 0.0671

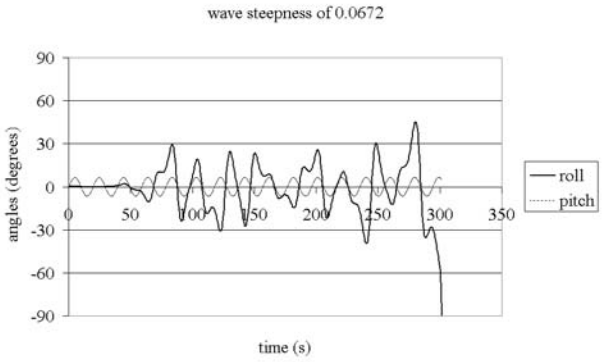

Fig. 12 Time series for the wave steepness of 0.0672

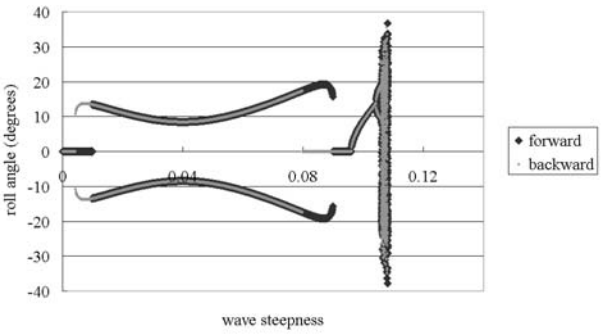

Fig. 13 Roll angles obtained by Poincare mapping with the time-varying restoring moment estimated from the captive model experiments.

So far the numerical analysis was carried out with the time-varying restoring moment calculated with the Froude-Krylov assumption.

However, this could overestimate the measured values. Thus, the same analysis was repeated but with the time-varying restoring moment obtained from the captive experiment. The results are shown in Fig. 13. The critical wave steepness for parametric rolling estimated with the captive experiment is 0.0097, and is smaller than that obtained with the Froude-Krylov assumption. Then the magnitude of the parametric rolling as a period-2 orbit firstly decreases and then increases with the wave steepness. The magnitude of the parametric rolling here is smaller than that in Fig. 8. At the wave steepness of 0.0898 the period-2 orbit disappears and then a period-1 orbit occurs. This period-1 orbit leads to period doubling bifurcation, chaos atractor and capsizing. The critical wave steepness for capsizing predicted with the captive experiment, 0.1081, is much larger than that with the Froude-Krylov prediction. More details of this geometrical study will be published in a separate paper.

4. ANALYTICAL APPROACH

The geometrical approach mentioned above requires an initial steady state for continuously tracing steady states. Thus, it is not so certain whether all stable states are identified or not. And it is not straightforward to identify unstable steady states in this approach. Thus, the authors applied an averaging method, one of analytical approach in nonlinear dynamics, [18] into Eq. (1). Here all steady states can be theoretically determined because steady states are solutions of algebraic equations. First, we assume the following solution of Eq. (1).

$$\phi = A\cos(\hat{\omega}t - \varepsilon) \tag{3}$$

Then, by assuming the following relationship to identify period-2 orbit,

$$\omega_e = 2\hat{\omega} \tag{4}$$

the averaging equation can be obtained as follows:

$$\begin{aligned}\dot{A} &= -\alpha A - \tfrac{3}{8}\gamma A^3\hat{\omega}^2 \\ &-\frac{1}{4}(\zeta_{ae}p_1 + \zeta_{ae}^2 p_2)A\{1-\frac{1}{2}(\frac{A}{\pi})^2\}\frac{\omega_\phi^2}{\hat{\omega}}\sin 2\varepsilon\end{aligned} \tag{5}$$

$$\begin{aligned}\dot{\varepsilon} &= \frac{\hat{\omega}}{2} \\ &-\frac{1}{2}\frac{\omega_\phi^2}{\hat{\omega}}[1+(\zeta_{ae}q_1+\zeta_{ae}^2 q_2+\zeta_{ae}^3 q_3)\{1-\frac{3}{4}(\frac{A}{\pi})^2\} \\ &+\frac{3}{4}l_3A^2+\frac{5}{8}l_5A^4] \\ &-\frac{1}{4}(\zeta_{ae}p_1+\zeta_{ae}^2p_2)\frac{\omega_\phi^2}{\hat{\omega}}\{1-(\frac{A}{\pi})^2\}\cos 2\varepsilon\end{aligned} \tag{6}$$

If we substitute zero into the left-hand sides of the above equations, steady states of the period-2 orbits can be obtained as their solutions. In this paper these are solved by the Bairstow method, which can algebraically determine all solutions. If we locally linearize these equations at their steady states, stability of the period-2 can be examined with their eigenvalues and their domain of attraction can be determined with their eigenvectors. [18] Hence these equations indicate that the existence of low cycle resonance and its stability does not depend on the exciting term. Thus, the effect of heading angle on low cycle resonance appears only in the magnitude of change of restoring moment due to waves. Since the change of restoring moment in pure following waves is almost largest, significant parametric rolling is more likely to occur when the heading angle is zero, and danger decreases with increasing heading angles in quartering waves. [19]

Numerical results from the above method for the case investigated with the geometrical method are shown in Fig. 14. Here the time-varying restoring moment are estimated

from the captive experiment. Comparison between this and Fig. 13 demonstrates that the analytical results for stable period-2 orbits are similar to those from the geometrical method. The critical wave steepness for the parametric rolling estimated by the averaging method well agrees with that from the Poincare map. And the layout of stable and unstable solutions proves that the disappearance of stable trivial solution is a sub-critical bifurcation. Once the parametric rolling occurs, its amplitude firstly decreases with the wave steepness and then increases. It becomes unstable at the wave steepness of 0.0838 and a stable trivial solution emerges. Here another subcritical bifurcation is found. The period-1 orbit found in Fig. 13 could be detected by repeating similar procedure for harmonic motions. However, for explaining chaos, averaging methods are limited in their ability. More details of the analytical studies will be published in a separate paper.

5. HEAD SEA CASE

So far, we investigated the loading condition marginally complying only with the general and weather criteria (3.1 and 3.2) of the IS Code. [20] If we apply the additional criteria for container ships greater than 100 metres, (4.9 of the IS Code), the centre of gravity should be significantly lowered as shown in Fig. 15 by possibly reducing the number of containers onboard significantly. This results in shorter natural roll period. As a result, the low cycle resonance could occur in head seas in place of following seas. For the subject ship, the natural roll period is 19.5 seconds and the low cycle resonance occurs when the ship runs at the Froude number of 0.114 in head seas according to a theory with linear restoring. [5]

The numerical results with the present geometrical method are shown for this operational condition in Fig. 16. In the range of the wave steepness from 0.01 to 0.02, the period-2 orbit can be found but its amplitude is very small. When the wave steepness exceeds 0.06, significant period-2 orbit, that is the low cycle resonance, suddenly develops and capsizing occurs at the wave steepness of 0.0733. The comparison with Fig. 8 suggests that the additional criteria for container ships could be effective for avoiding the parametric rolling in moderate sea state but does not decrease danger of capsizing associated with parametric rolling despite significant loss of its profitability.

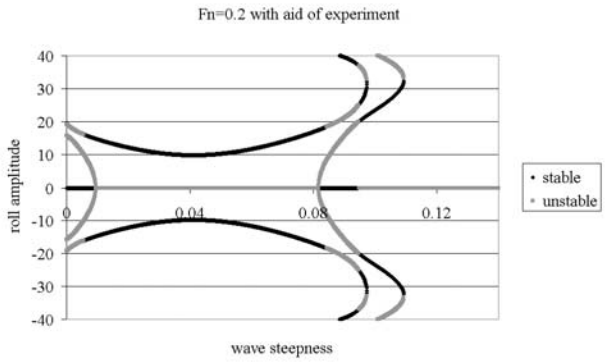

Fig. 14 Period-2 roll amplitude calculated by the averaging method with the time-varying restoring moment estimated from the captive model experiments.

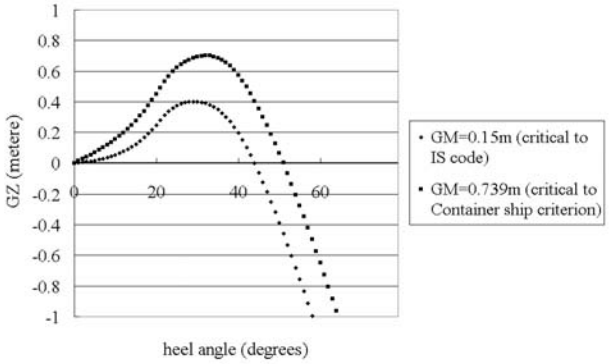

Fig. 15 Comparison of restoring arm curves in calm water.

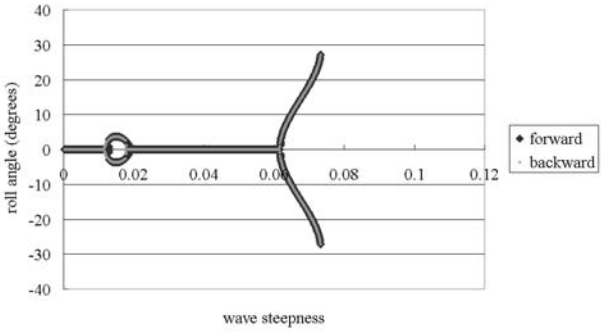

Fig. 16 Roll angles obtained by Poincare mapping with the time-varying restoring moment calculated with the Froude-Krylov assumption for the ship marginall complying with the container ship criteria.

6. CONCLUSIONS

Parametric rolling is investigated with realistic restoring moment in waves by experimental, geometrical and analytical methods. The conclusions are listed below.

1) The Froude-Krylov prediction could overestimate the wave effect on roll restoring moment, and could overestimate a danger of capsizing associated with parametric rolling.

2) Parametric rolling could often accompany with subcritical bifurcation, period-doubling, symmetry breaking, chaos and capsizing.

3) An averaging method is useful to more efficiently identify subcritical bifurcation as an onset of parametric roll resonance and a geometrical method is effective for identifying chaos.

4) Increase of the metacentric height only, such as the container ship criteria of the IMO IS Code, could shift the parametric roll resonance zone from following seas to head seas but does not significantly decrease a danger of capsizing associated with parametric roll resonance.

7. ACKNOWLEDGEMENTS

Some parts of the work described here were carried out during the first and second authors' stays at Universities of Glasgow and Strathclyde, which were supported by Japan's Ministry of Education, Culture, Sports, Science and Technology as well as its Grant-in-Aid (No. 15360465). The work was partly carried out as a research activity of the RR-S2 research panel of the Shipbuilding Research Association of Japan, funded by the Nippon Foundation. The authors express their sincere gratitude to the above organisations.

8. REFERENCES

[1]. Umeda, N., Hamamolto, M. et al., Model Experiments of Ship Capsize in Astern Seas, J Soc. Naval Architects Japan, 177, 207-217, 1995.

[2]. France, W.N., Levadou, M. et al., An Investigation of Head-Sea Parametric Rolling and Its Influence on Container Lashing System, Marine Technology, 40(1), 1-19, 2003.

[3]. SLF Sub-Committee, Report to the Maritime Safety Committee, SLF 45/14, IMO (London), 2002.

[4]. Watanabe, Y., On the Dynamic Properties of the Transverse Instability of a Ship Due to Pitching (in Japanese), J. Soc. Naval Architects Japan, 53, 51-70, 1934.

[5]. Kerwin, J.E., Note on Rolling in Longitudinal Waves, Int. Shipbuilding Progress, 2(16), 597-614, 1955.

[6]. Sanchez, N.E. and Nayfeh, A.H., Nonlinear Rolling Motions of Ships in Longitudinal Waves, Int. Shipbuilding Progress, 37(411), 247-272, 1990.

[7]. Kan, M. and Taguchi, H., Capsizing of a Ship in Quartering Seas (Part 4. Chaos and Fractals in Forced Mathieu Type Capsizing Equation) (in Japanese), J. Soc. Naval Architects Japan, 171, 229-244, 1992.

[8]. Soliman, M. and Thompson, J.M.T., Indeterminate Sub-Critical Bifurcations in Parametric Resonance, Proc. R. Soc. Lond. A, 438, 511-518, 1992.

[9]. Oh, I.G., Nayfeh, A.H. and Mook, D.T., A Theoretical and Experimental Investigation of Indirectly Excited Roll Motion in Ships, Phil. Trans. R. Soc. Lond. A., 358, 1731-1881, 2000.

[10]. Munif, A. and Umeda, N., Modeling Extreme Roll Motions and Capsizing of a Moderate-Speed Ship in Astern Waves, J. Soc. Naval Architects Japan, 187, 51-58, 2000.

[11]. Paulling, J.R., The Transverse Stability of a Ship in a Longitudinal Seaway, J. Ship Research, 4(4), 37-49, 1961.

[12]. Hamamoto, M. and Nomoto, K., Transverse Stability of a Ship in a Following Sea, Proc. 2nd Int. Conf. Stability Ships Ocean Vehicles, Soc. Naval Architects Japan (Tokyo), 215-224, 1982.

[13]. Umeda, N. and Yamakoshi, Y., Experimental Study on Pure Loss of Stability in Regular and Irregular Following Seas, Proc. 3rd Int. Conf. Stability Ships Ocean Vehicles, Tech Uni Gdansk, 1, 93-99, 1986.

[14]. Umeda, N., Hashimoto, H. and A. Matsuda, Broaching Prediction in the Light of an Enhanced Mathematical Model, with Higher-Order Terms Taken into Account, J. Marine Science and Technology, 7, 145-155, 2003.

[15]. Umeda, N. and Renilson, M.R., Benchmark Testing of Numerical Prediction on Capsizing of Intact Ships in Following and Quartering Seas, Proc. 5th Int. Workshop Ship Stability Operational Safety, Uni Trieste, 6.1.1-6.1.10, 2001.

[16]. Grim, O., Beitrag zu dem Problem der Sicherheit des Schiffes im Seegang, Schiff und Hafen, 6, 490-497, 1961.

[17]. Thompson, J.M.T. and Stuart, H.B., Nonlinear Dynamics and Chaos, 2nd Edition, John Wiley & Sons (Chichester), 2002.

[18]. Guckenheimer J. and Holmes, P., Nonlinear Oscillations, Dynamical Systems, and Bifurcations of Vector Fields, Springer-Verlag (New York), 1990.

[19]. Umeda, N. and Hamamoto, M., Capsize of Ship Models in Following / Quartering Waves: Physical Experiments and Nonlinear Dynamics, Phil. Trans. R. Soc. Lond. A., 358, 1883-1904, 2000.

[20]. IMO, Code on Intact Stability for All Types of Ships Covered by IMO Instruments, 2nd Edition, IMO (London), 2002.